

Contrasts in variations of the carbon and oxygen isotopic composition of travertines formed in pools and a ramp stream at Huanglong Ravine, China: Implications for paleoclimatic interpretations

Haijing Wang^{a,b,1}, Hao Yan^{a,1}, Zaihua Liu^{a,*}

^a State Key Laboratory of Environmental Geochemistry, Institute of Geochemistry, Chinese Academy of Sciences, Guiyang 550002, China

^b Department of Geography, Zhengzhou Normal University, Zhengzhou 450044, China

Received 27 May 2013; accepted in revised form 1 October 2013; available online 18 October 2013

Abstract

Water samples and modern endogenic (thermogene) travertine calcite deposited on plexiglass substrates in travertine pools and a ramp stream were collected along the Huanglong Ravine, Sichuan, SW China at regular ~10 day intervals from early May to early November in 2010, including both wet and dry conditions. Temporal and spatial variations in the $\delta^{13}\text{C}$ and $\delta^{18}\text{O}$ values of the modern travertine were examined to understand their potential for paleoclimatic and paleoenvironmental interpretations. It was found that $\delta^{13}\text{C}$ and $\delta^{18}\text{O}$ of travertine formed in the ramp stream were low in the warm rainy season and high in the cold dry season. Their positive correlation was mainly due to dilution and rainfall seasonal effects on $\delta^{13}\text{C}$ and $\delta^{18}\text{O}$ values, respectively, i.e., low $\delta^{13}\text{C}$ values were caused by dilution by overland flow with depleted $\delta^{13}\text{C}$ values and reduced CO_2 -degassing in the warm rainy season while low $\delta^{18}\text{O}$ values of travertine were because of low $\delta^{18}\text{O}$ values of water induced by seasonal variation in oxygen isotopic ratios of rainwater. Meanwhile, kinetic effect on oxygen isotopic fractionation during ramp travertine deposition existed and reduced this positive correlation. In contrast, the $\delta^{13}\text{C}$ and $\delta^{18}\text{O}$ values of the pool travertines displayed a converse behavior which was caused mainly by the temperature effect. Low $\delta^{18}\text{O}$ values and high $\delta^{13}\text{C}$ values in the warm rainy season were correlated chiefly with the higher water temperatures. Therefore, the $\delta^{13}\text{C}$ and $\delta^{18}\text{O}$ values of the travertine may be used for paleo-rainfall or paleotemperature reconstruction respectively. This study demonstrates that endogenic travertine, like epigenic (meteogene) tufa, may be a suitable candidate for high-resolution paleoclimatic and paleoenvironmental reconstructions. However, since travertines deposited under differing hydrodynamic conditions (e.g., pools with still water contrasted to fast flow streams) have different climatic responses, it is necessary to check the depositional facies of fossil travertine samples before they can be used for palaeoclimate (temperature and/or rainfall) reconstruction.

© 2013 Elsevier Ltd. All rights reserved.

1. INTRODUCTION

High-resolution terrestrial records are highly required in the paleoclimatic research. Among the various terrestrial records, speleothems have been of particular interest in studies of Quaternary climate change in recent years (e.g.,

Wang et al., 2001, 2008; McDermott, 2004; Yuan et al., 2004). Speleothems from across a wide range of climatic zones may provide long, continuous, and commonly well-preserved records, and can be accurately dated over the last several hundred thousand years.

Like speleothems, travertine/tufa deposited at the surface in karst areas can also be an important geological archive for terrestrial paleoclimatic studies (Andrews and Brasier, 2005; Andrews, 2006; Liu et al., 2006; Sun and Liu, 2010). In particular, because of the high depositional

* Corresponding author. Tel.: +86 851 5895263.

E-mail address: liuzaihua@vip.gyig.ac.cn (Z. Liu).

¹ These authors contributed equally to this work.

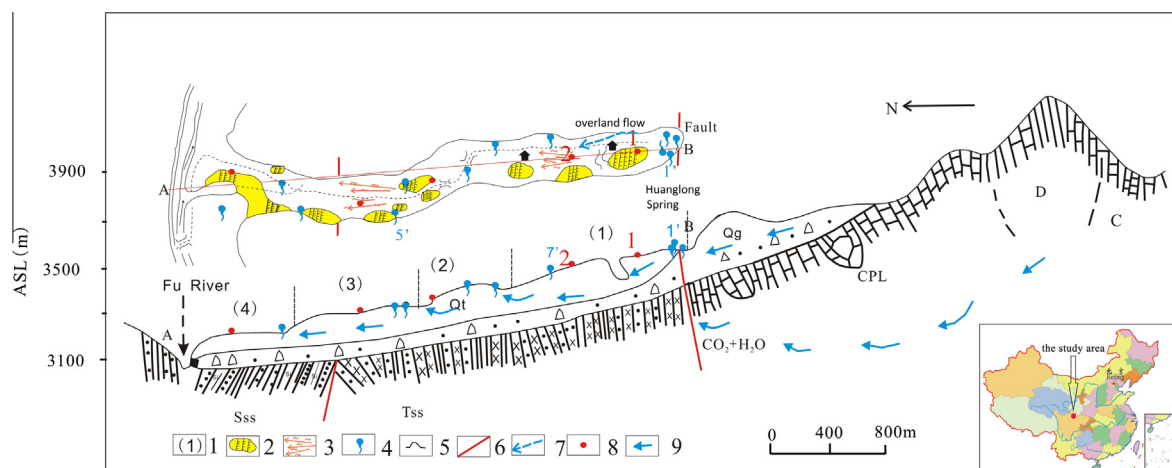


Fig. 1. Geological plan and section of Huanglong Ravine, showing the sampling sites (modified after Zhang et al., 2012). 1. No. of the subsystem; 2. Rimstone dam and pool travertine; 3. Stream ramp travertine; 4. Spring; 5. Travertine cave; 6. Fault; 7. Overland flow (surface water); 8. Sampling site; 9. Direction of groundwater flow. Qt/Qg-Quaternary travertine/glacial sand and gravel; Tss-Triassic sandstone and slate; CPL – Carboniferous and Permian limestone; C – Carboniferous limestone; D – Devonian slate and limestone; Sss – Silurian slate, intercalated with sandstone.

rates (mm to cm per year, Kano et al., 2003; Kawai et al., 2009; Liu et al., 2010), high-resolution (up to seasonal, monthly or even daily) paleoclimatic information can be obtained. Before using travertines or tufas to reconstruct climate changes, however, one must understand the cause of variations in the geochemical proxies (chiefly stable oxygen and carbon isotope compositions) in these precipitates, and the quantitative relationships between these proxies and climatic and environmental factors (Andrews et al., 1997; Andrews and Brasier, 2005; Andrews, 2006).

The climatic interpretation of proxies in travertine/tufa and their controlling mechanisms are generally complicated and often site-specific. Matsuoka et al. (2001) studied an annually laminated tufa from Shirokawa, SW Japan, and found that the variation of $\delta^{18}\text{O}$ reflected seasonal changes in water temperature while $\delta^{13}\text{C}$ variations were controlled by seasonal changes in the $\delta^{13}\text{C}$ of dissolved inorganic carbon in the groundwater. Liu et al. (2006) found the co-variations of $\delta^{18}\text{O}$ and $\delta^{13}\text{C}$ values recorded in a laminated travertine from Baishuitai, SW China, are caused by seasonal changes in rainfall, i.e., low $\delta^{18}\text{O}$ and $\delta^{13}\text{C}$ values during the warm and rainy seasons are related to the rainfall amount effects in this subtropical monsoonal region, and dilution of overland flow after rainfall. Yan et al. (2012) investigated the oxygen isotope composition in two travertine-depositing systems with differing hydrodynamic conditions at Baishuitai, and showed that $\delta^{18}\text{O}$ values in travertine deposited in a channel with fast flow were related to the rainfall whereas $\delta^{18}\text{O}$ values in travertine deposited in pools with slow flow can be used to estimate water temperatures. Therefore, direct transfer of the relationships between proxies and climatic factors from one site to another, as reported in some previous studies, may result in incorrect interpretation due to the complexity of the mechanisms controlling these proxies.

Huanglong Ravine, Sichuan, SW China, is internationally known for its unusual and diversified landscapes (e.g., travertine pools, travertine falls and flowstones) and

was listed by UNESCO in 1992 in the World's Nature Heritage. Travertine here has been studied more than 20 years. Most of the previous studies focused on the variation of hydrochemistry and precipitation mechanism of travertine (e.g., Liu et al., 1995; Yoshimura et al., 2004; Wang et al., 2010; Zhang et al., 2012). Liu et al. (1995) placed small rectangular shaped tablets of pure marble under different flow regimes and found that deposition rates in fast flowing water were four times higher compared to still water, indicating a strong influence of hydrodynamics. Zhang et al. (2012) reexamined travertine deposition rates using a similar method and found that the travertine deposition rates in Huanglong Ravine have declined significantly during past 20 years. They suggested that the reduction in travertine deposition most likely resulted from the phosphate pollution caused by the tourism activities. Yoshimura et al. (2004) investigated the chemical compositions together with stable oxygen and carbon isotope ratios to evaluate the evaporation and the contribution of deep source CO_2 to dissolved carbonates in spring water. However, the potential paleoclimatic significance of the stable oxygen and carbon isotopic composition of the travertine in Huanglong Ravine has not been studied hitherto. The purpose of this report is (1) to examine both the seasonal and spatial variations in $\delta^{13}\text{C}$ and $\delta^{18}\text{O}$ values of the modern endogenic travertine at Huanglong Ravine; (2) to understand the climatic implications of the stable isotope records of travertines deposited under different hydrodynamic conditions (pools with still water compared to streams with rapid flow), and (3) to compare with the data obtained at another travertine site at Baishuitai, Yunnan, SW China (e.g., Sun and Liu, 2010; Yan et al., 2012).

2. GENERAL SETTING OF THE STUDY AREA

Huanglong Ravine is located about 360 km NW of the provincial capital, Chengdu, Sichuan Province, on the southern slopes of the Minshan Mountains that separate

the Qinghai Highlands from the Sichuan Basin. Its elevation ranges from 3100 to 3600 m above sea level (asl). The geology consists of Paleozoic carbonate rocks exceeding 4000 m in thickness, overlain by about 1000 m of Mesozoic clastic rocks plus Cenozoic alluvial gravels, glacial moraines and travertine (Liu et al., 1995). In the Ravine, the travertine deposits have accumulated over a width of ~250 m for a length of 3.5 km in the major forms of pool travertine and ramp travertine (Fig. 1). Downstream continuous exchange between surface water and groundwater makes the aqueous flow systems of Huanglong Ravine extremely complex, being divisible into four subsystems (Fig. 1, for details, see Zhang et al., 2012). We selected the first subsystem at Wucaichi pools (Site No. 1, Fig. 1) and Matihai ramp stream (Site No. 2, Fig. 1) to examine the spatial–temporal changes of the geochemical proxies and the underlying mechanisms.

The average annual precipitation at Huanglong Spring is 759 mm, about 72% of it occurring during the rainy season from May to September. The mean air temperature is 1.1 °C. Groundwater (Huanglong spring) issues along a fault zone at an altitude of about 3580 m asl, with a water temperature about 5 °C higher than that of annual mean air temperature. The Huanglong spring water (with high Ca^{2+} and HCO_3^- concentrations) fed Wucaichi travertine pools (Multi-colored Pools, sampling site No. 1 in Figs. 1 and 2a). After the water spills over the lip of the rimstone dam, it mixed with surface water (overland flow) containing soil water and glacier-snowmelt water from higher mountains (including the highest peak, Xuebaoding, 5588 m asl) (Fig. 2a). The overland flow had low concentrations of Ca^{2+} and HCO_3^- . This mixture of spring water and overland flow then supplied the Matihai ramp section with a steep slope (sampling site No. 2 in Figs. 1 and 2b). Because the flow of Huanglong spring is relatively stable, change in the flow rate at the ramp was mainly related to the mixture of surface flow.

3. METHODS

3.1. Installation and collection of plexiglass substrates and isotope measurement of modern travertine and water samples

In order to obtain modern endogenic travertine samples for isotope measurement, 5×5 cm plexiglass substrates for depositing travertine were placed in the water at the monitoring sites (Zhang et al., 2012). The substrates were oriented parallel to the water surface and located in fast flowing stream water, 2 cm below the water surface, while others were mounted 10 cm beneath the water surface in pools with standing water (Zhang et al., 2012).

The substrates were replaced about every 10 days; after collection each plexiglass substrate was dried at 50 °C for a period of 24 h and cooled to room temperature in a glass dryer. The amount of travertine deposited on them was determined by measuring the weight increase of the plexiglass substrate. The stable isotopic composition of carbon and oxygen ($\delta^{13}\text{C}$ and $\delta^{18}\text{O}$) on the travertine samples were measured in the State Key Laboratory of Environmental Geochemistry, Guiyang, China. Each sample was put into a vial to react with pure H_3PO_4 . The CO_2 generated was

then purified and sent to an MAT-252 mass spectrometer for measurement. The results were reported as ‰ vs. Vienna Pee Dee Belemnite (VPDB). The standard deviation of isotopic measurements performed is 0.15‰ for $\delta^{13}\text{C}$ value and 0.20‰ for $\delta^{18}\text{O}$ value.

When the travertine samples were being collected, water samples were taken alongside the plexiglass collectors by syringe with 0.45 μm Minisart filters. The water samples for $\delta^{18}\text{O}$ value measurement were stored in 60 ml polyethylene bottles that were filled completely to prevent evaporation and measured by the GV IsoPrime IRMS after the water sample was equilibrated with CO_2 gas in a vial. The standard deviation of $\delta^{18}\text{O}$ value measurements performed is 0.20‰.

3.2. Measurement of the water chemistry

Water temperature, pH and specific conductivity at each monitoring site were measured *in situ* daily with a hand-held water quality data logger, Model WTW 350i, with resolution of 0.05 pH, 0.1 °C and 1 $\mu\text{S}/\text{cm}$, respectively (Liu et al., 2010). Electrodes were calibrated prior to use with pH 7 and 10, and conductivity (1412 $\mu\text{S}/\text{cm}$) standards. *In situ* titration was used to determine $[\text{HCO}_3^-]$ and $[\text{Ca}^{2+}]$ approximately every 10 days by the Aquamerck Alkalinity Test and Hardness Test. The resolutions are 6 and 1 mg/L, respectively (Liu et al., 2010). In pure limestone areas, as is the case in this study, specific conductivity fluctuations in a travertine depositing stream can be attributed solely to Ca^{2+} and HCO_3^- changes, either by calcite deposition or dissolution (e.g., Liu et al., 2004; Krawczyk and Ford, 2006; Wang et al., 2010) or by dilution with rain water or snowmelt water. Paired Ca^{2+} (or HCO_3^-) and conductivity values were correlated and regression was used to establish a time-series of Ca^{2+} and HCO_3^- changes. At Huanglong, these concentrations are linearly related to specific conductivity by the relationships (Wang et al., 2010):

$$[\text{Ca}^{2+}] = 0.2651\text{SpC} - 18.607; \quad r^2 = 0.9948 \quad (1)$$

$$[\text{HCO}_3^-] = 0.8017\text{SpC} - 54.827; \quad r^2 = 0.9951 \quad (2)$$

where brackets denote species concentrations in mg/L and SpC is specific conductivity in $\mu\text{S}/\text{cm}$ at 25 °C.

The water samples were analyzed in the State Key Laboratory of Environmental Geochemistry. Concentrations of K^+ , Na^+ and Mg^{2+} were determined by Inductively Coupled Plasma Optical Emission Spectrometry (Model Vista MPX) and those of Cl^- , PO_4^{3-} and SO_4^{2-} by ion chromatography (Model ICS-90) (Liu et al., 2010).

3.3. Rainfall recording and collection and isotope measurement of rainwater and the spring water

The rainfall was recorded every 15 min with a resolution of 0.2 mm with a HOBO rain gauge in Huanglong Ravine and the data were stored in a HOBO 4-channel data logger. This information is used to investigate the climatic control on the water chemistry and the stable isotopes of the travertine.

Polyethylene funnels were used for rainwater collection, being cleaned by the rainwater at the beginning of

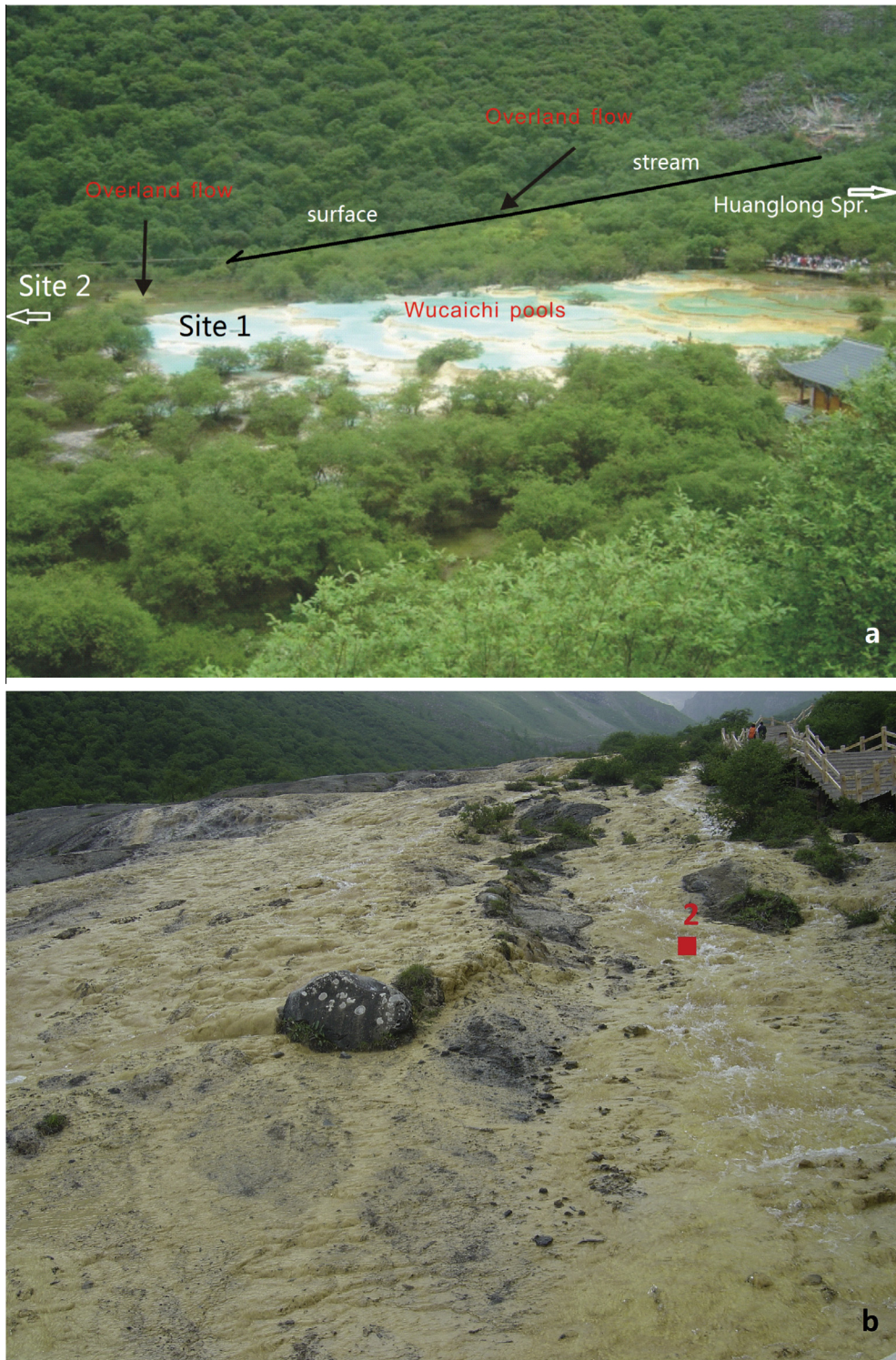


Fig. 2. Photograph of the two experimental sites (Nos. 1 and 2) with deposits of pool travertine (a) and ramp travertine (b).

each rain event. After the rain stopped, the accumulated rainwater was collected in a 60 ml polyethylene bottle that was filled completely to prevent evaporation. The $\delta^{18}\text{O}$ values of rainwater and spring water samples were measured by the GV IsoPrime IRMS, as with the

stream water samples. The δD values of water were measured by GV IsoPrime IRMS after each water sample was equilibrated with H_2 gas using platinum wire as a catalyst in a vial. The standard deviation of δD measurements is 2‰.

4. RESULTS

4.1. Isotopic composition of rainwater and overland flow

The δD and $\delta^{18}O$ values of rainwater ranged between -37‰ and -6.1‰ in the dry season to -190‰ and -26.1‰ in the rainy season (Table 1, only $\delta^{18}O$ values are shown). Generally, there was a depleted trend in $\delta^{18}O$ values of rainwater during the study time. This may reflect the seasonal variation in $\delta^{18}O$ values of rainwater in the study area (Zhang et al., 2002). The large range of δD and $\delta^{18}O$ values of rainwater makes mountainous continental interior sites such as Huanglong Ravine particularly well suitable for studies of seasonal variations in isotope ratios in calcite precipitation. There was no obvious correlation between rainfall amount and the $\delta^{18}O$ values. Several overland flow samples were taken to investigate the $\delta^{18}O$ values (Table 2). There was also a decreasing trend in $\delta^{18}O$ values, as seen in $\delta^{18}O$ values of rainwater. Thus it is expected that it was the seasonal change in $\delta^{18}O$ values of rainwater that induced the temporal variation in $\delta^{18}O$ values of overland flow. This provides a theoretical basis for interpretation of temporal variation in travertine $\delta^{18}O$ values at Matihai ramp section.

4.2. General hydrochemical and stable isotopic features of Huanglong Spring

The general hydrochemical composition of the Huanglong Spring which feeds the sample pools and some of the

stream water studied is simple; Ca^{2+} was the major cation with a molarity percentage of $>95\%$, and HCO_3^- the major anion in with a molarity percentage of $>90\%$ (Wang et al., 2010). Thus, the hydrochemical type was HCO_3-Ca , reflecting the predominant control of the Carboniferous-Permian carbonate bedrock at the site. The spring had high concentrations of Ca^{2+} and HCO_3^- , high CO_2 pressures ($>13,000$ pa) and higher temperature relative to annual mean of air temperature, which are not likely to be produced by biological activity in the soil alone (about 250 and 750 mg/l, Wang et al., 2010). According to Liu et al. (2000) and Yoshimura et al. (2004), the CO_2 in the Huanglong Spring was mainly endogenic. The $\delta^{18}O$ and $\delta^{13}C_{DIC}$ values of the spring water were about -12.34‰ and 0.0‰ , respectively, and were relatively stable, showing no seasonal change. Such high values of $\delta^{13}C_{DIC}$ are never expected in epigenic settings, and thus are further evidence for the endogenic origin of the CO_2 . However, the spring water was meteoric origin according to the isotopic characteristics of hydrogen and oxygen (Wang et al., 2012).

4.3. Temporal variations of water chemistry of the pool and the ramp stream

Fig. 3a and b show respectively the hydrochemical variations at Sample Site No. 1 (the uppermost colorful travertine pool) and No. 2 (the ramp travertine site) from May 20 to Nov. 20, 2010. It can be seen that water temperatures at two sites displayed a seasonal pattern following to the change in air temperature; higher in summer and lower in

Table 1
The amount and $\delta^{18}O$ values of rainwater collected in Huanglong Ravine.

Date	Rainfall (mm)	$\delta^{18}O_{rain}$ (VSMOW. ‰)	Date	Rainfall (mm)	$\delta^{18}O_{rain}$ (VSMOW. ‰)	Date	Rainfall (mm)	$\delta^{18}O_{rain}$ (VSMOW. ‰)
2010/05/21	11.4	-8.20	2010/07/15	2.6	-11.52	2010/09/22	3.0	-16.67
2010/05/26	24.0	-12.04	2010/07/16	18.6	-13.84	2010/09/25	9.4	-23.60
2010/05/31	13.4	-13.74	2010/07/31	0.2	-10.61	2010/09/27	2.2	-17.58
2010/06/02	12.6	-19.99	2010/08/03	0.8	-13.54	2010/09/30	3.6	-7.81
2010/06/09	3.6	-11.53	2010/08/05	2.8	-13.37	2010/10/01	14.4	-19.38
2010/06/18	6.4	-6.05	2010/08/13	5.4	-14.58	2010/10/11	0.2	-26.07
2010/06/25	2.4	-6.80	2010/08/16	6.0	-9.00	2010/10/13	4.8	-14.91
2010/06/30	7.2	-13.97	2010/08/18	2.0	-12.48	2010/10/18	4.0	-10.40
2010/07/02	0.6	-10.03	2010/08/22	0.4	-17.74	2010/10/19	2.4	-11.79
2010/07/03	10.4	-12.07	2010/08/25	4.6	-15.02	2010/10/24	2.8	-14.38
2010/07/04	2.2	-10.63	2010/08/30	21.4	-19.47	2010/10/28	1.6	-14.20
2010/07/07	1.4	-6.48	2010/09/01	9.2	-10.94	2010/10/29	6.2	-17.85
2010/07/09	6.4	-11.22	2010/09/08	14.0	-15.61	2010/11/02	4.0	-17.56
2010/07/12	6.8	-10.18	2010/09/21	4.0	-16.82			

Table 2
The $\delta^{18}O$ values of overland flow collected in Huanglong Ravine.

Date	$\delta^{18}O$ (VSMOW. ‰)	Date	$\delta^{18}O$ (VSMOW. ‰)
2010/04/27	-12.28	2010/09/08	-13.11
2010/05/20	-12.16	2010/09/26	-12.93
2010/06/02	-12.24	2010/10/06	-12.80
2010/07/07	-12.85	2010/10/16	-12.80
2010/07/16	-12.69	2010/10/26	-13.06
2010/08/28	-12.82	2010/11/06	-12.97

spring and autumn (Fig. 3). The pH value and SIc (saturation index of calcite) at Site No. 1 did not show synchronous changes with rain events, with the mean value of 7.91 and 1.25, respectively (Fig. 3a). Ca concentration in pool water also remained relatively stable with the mean value and standard deviation 208 ± 8 mg/L. The low value of Ca concentration around early June and especially July 20 might be due to the combination effect of continuous heavy rain during that period and inflow of snow-molten water. Because of the short distance between Huanglong Spring and this site No. 1 (Fig. 1), the dilution effect of rainwater was not strong enough to disturb the aqueous geochemical properties such as pH value and Ca concentration. This is indicated by no correlation between them and rainfall ($R = -0.003$ and -0.06 for pH value and Ca concentration respectively). However, $p\text{CO}_2$ and water temperature at Site No. 1 showed detectable temporal variations with the values of 616 ± 156 Pa and 10.2 ± 3.5 °C, and correlated with each other ($R = 0.74$).

In contrast, values of Ca concentration, $p\text{CO}_2$ and SIc of the ramp stream water at Site No. 2 were more variable (109 ± 18 mg/L, 145 ± 38 Pa and 1.11 ± 0.13 , respectively) and clearly decreased during the rainy period (Fig. 3b). There is a negative correlation between the hydrochemistry and quantities of rain at Site No.2, indicating dilution by overland flow. This is illustrated by the large decreases of Ca^{2+} , pH and SIc after rainfall events, especially on June 8, July 15, August 21 and October 3 (Fig. 3b). After the middle of October the rain stopped, air temperatures fell to 0 °C and any precipitation was in the form of snow. As a consequence a general increasing trend can be seen in $[\text{Ca}^{2+}]$ and $p\text{CO}_2$ (Fig. 3b).

4.4. Contrasts in temporal variations of the $\delta^{13}\text{C}$ and $\delta^{18}\text{O}$ values in the pool and ramp travertines

Figs. 4 and 5 show the temporal variations of the $\delta^{18}\text{O}$ and $\delta^{13}\text{C}$ values of the pool travertine at Site 1 and the ramp travertine at Site 2 respectively. For Site No. 1, $\delta^{18}\text{O}$ value of travertine decreased first from June to the lowest value at the beginning of August when water temperature is the highest. Then it increased from -11.95‰ in August to -9.98‰ in November. It is seen that the $\delta^{18}\text{O}$ values of the pool travertine showed negative correlation with water temperature while $\delta^{18}\text{O}$ values of water did not display obvious temporal variation ($-12.08 \pm 0.26\text{‰}$) (Fig. 4). The $\delta^{13}\text{C}$ values of pool travertine showed synchronous change with the temperature generally.

In contrast, in the ramp travertine deposited at Site No. 2, $\delta^{13}\text{C}$ values increased from 2.73‰ on June 2, 2010 to 4.55‰ on August 8, 2010, and decreased during the period of heavy rain, then rose up gradually. Statistic analysis shows that the $\delta^{13}\text{C}$ values of ramp travertine positively correlated with $p\text{CO}_2$ ($R = 0.63$) and negatively correlated with rainfall ($R = -0.68$). The $\delta^{18}\text{O}$ values of ramp travertine did not show obvious co-variation with rainfall (Table 3) when the $\delta^{18}\text{O}$ values of ramp stream water here showed a similar trend with those of overland flow and rainwater.

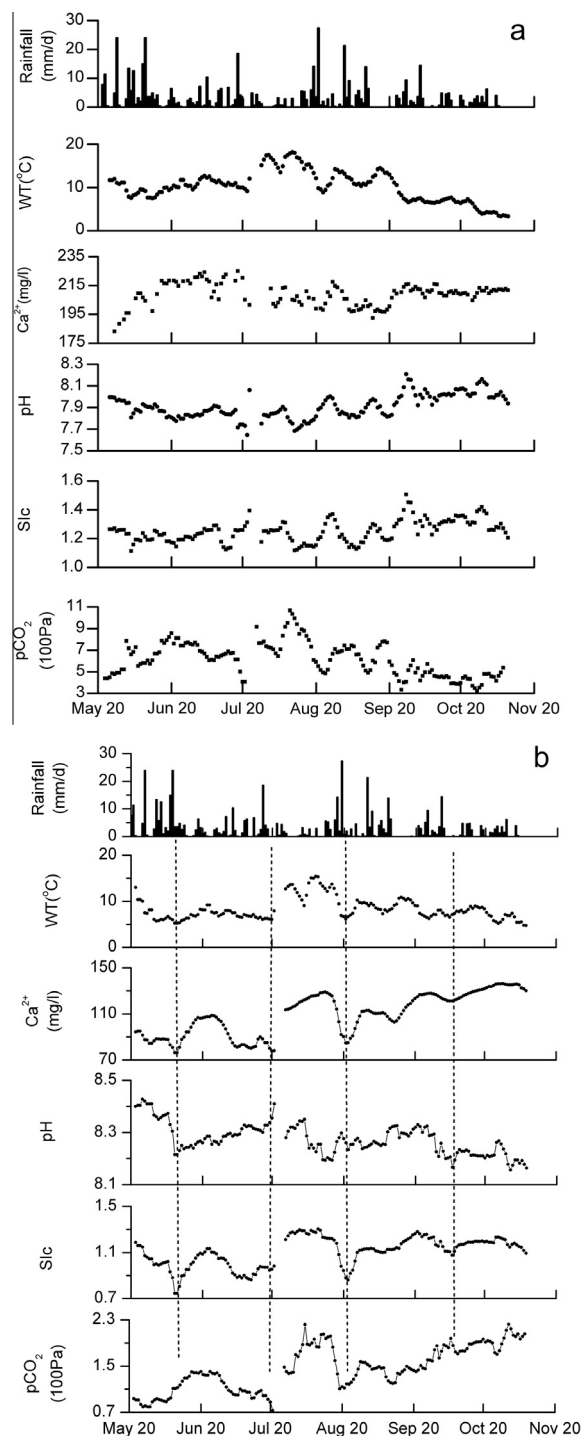


Fig. 3. Hydrochemical variations at Site 1 in the travertine pool (a) and Site 2 in the travertine ramp (b) for the period, May 20–Nov. 20, 2010, including wet and dry seasons.

4.5. Contrasts in spatial variations of the $\delta^{13}\text{C}$ and $\delta^{18}\text{O}$ values of the pool and ramp travertines

Figs. 6 and 7 show the spatial variations in the $\delta^{13}\text{C}$ and $\delta^{18}\text{O}$ values of the ramp and pool travertine samples respectively, which were collected in July and November in order

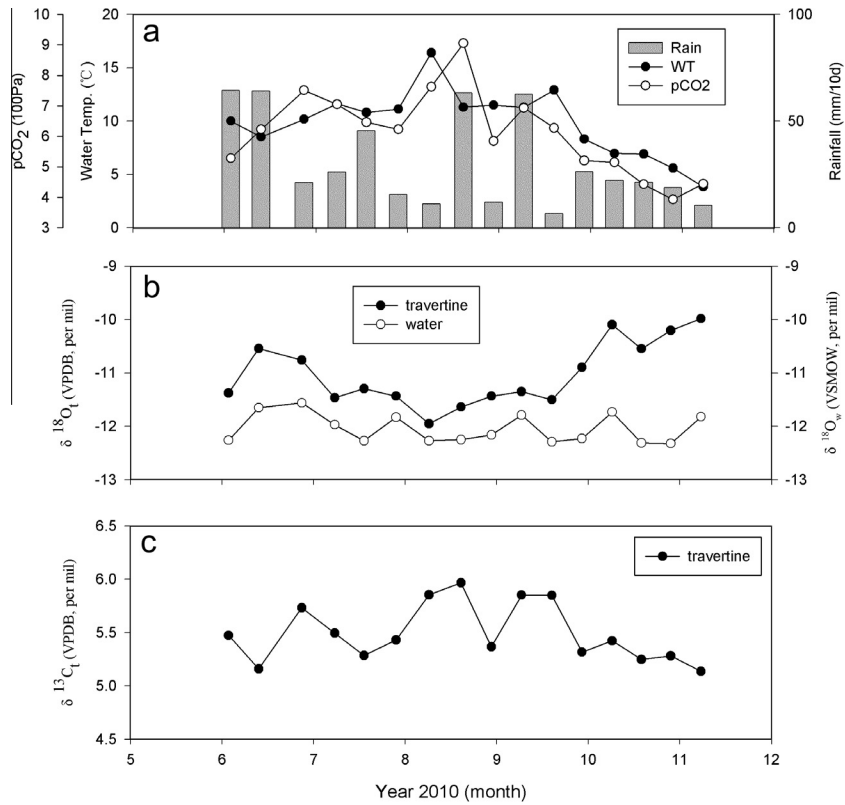


Fig. 4. Temporal variations in the $\delta^{18}\text{O}$ values of the water and travertine samples (b) and $\delta^{13}\text{C}$ values of travertine (c) at Wucaichi pool (Site No. 1), in relation to changes in coeval water temperature, pCO_2 and rainfall (a).

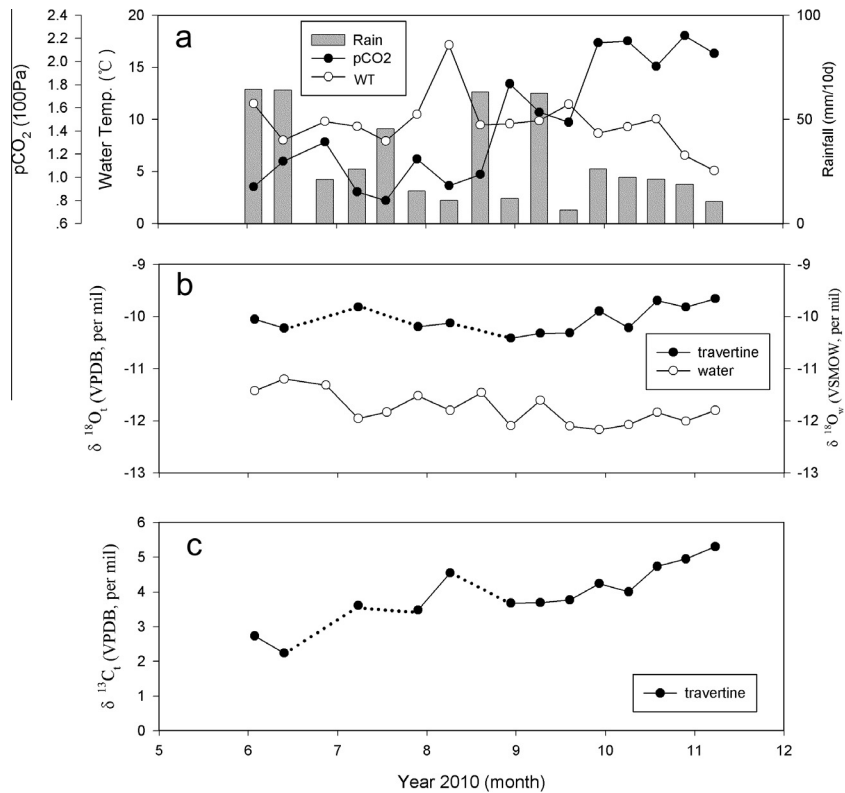


Fig. 5. Temporal variations in the $\delta^{18}\text{O}$ values of the water and travertine samples (b) and $\delta^{13}\text{C}$ values of travertine (c) at Matihai ramp (Site No. 2), in relation to changes in coeval water temperature, pCO_2 and rainfall (a).

Table 3

Statistical relationships between isotopic compositions of travertine and water temperature, rainfall and pCO₂ in Huanglong Ravine.

Isotopes	Site	R_T	P	R_P	P	R_{pCO_2}	P
$\delta^{18}O_t$	No. 1	-0.93	<0.0001	-0.16	0.5578	0.70	0.0024
	No. 2	-0.40	0.1795	-0.19	0.5402	0.28	0.3626
$\delta^{13}C_t$	No. 1	0.72	0.0018	0.12	0.6508	0.77	0.0005
	No. 2	-0.17	0.5631	-0.68	0.0103	0.63	0.0218

R_T : Coefficient for water temperature; R_P : Coefficient for rainfall; R_{pCO_2} : Coefficient for pCO₂; P : Significance level.

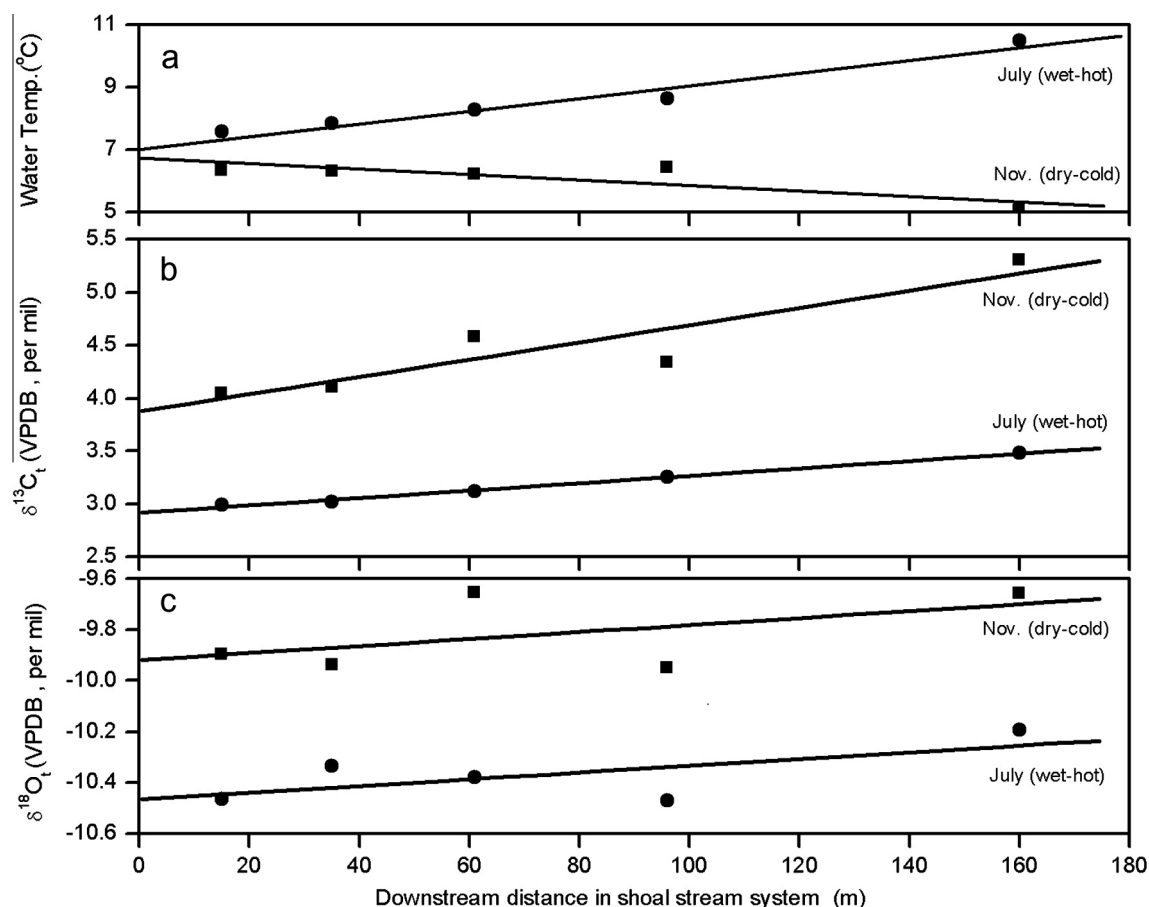


Fig. 6. Spatial variation in the $\delta^{13}C$ (b) and $\delta^{18}O$ (c) values of ramp travertine under wet (July) and dry (November) conditions at Huanglong Ravine, in relation to changes in the coeval water temperature (a).

to represent the wet period and the dry period at Huanglong Ravine.

It is seen that the ramp travertine $\delta^{13}C$ values show a general increasing trend downstream. The increase of slope was steeper in the dry season (Nov) than in the wet season (July) when the dilution effect was weaker in dry season than in wet season (Fig. 6b).

In contrast, the pool travertine $\delta^{18}O$ values decreased downstream during the warm-wet season (July) and increased downstream during the cold-dry season (Fig. 7c). This may be caused by the spatial variations of water temperature with flow across the pools (Fig. 7a) due to the temperature effect when travertine is precipitated in isotopic equilibrium (see further discussion below).

5. DISCUSSION

5.1. Dilution effects and rainfall amount effects on the variations in the $\delta^{13}C$ and $\delta^{18}O$ values of the ramp travertine: implications for reconstruction of paleo-rainfall

Sun and Liu (2010) investigated the seasonal variations in the $\delta^{13}C$ and $\delta^{18}O$ values of the modern endogenic (thermogene) travertine deposited in a channel at Baishuitai, Yunnan, SW China. Their results showed that both $\delta^{13}C$ and $\delta^{18}O$ values of the travertine were low in the warm rainy season and high in the cold dry season, which is similar to the data of the ramp travertine at Site 2 in this study.

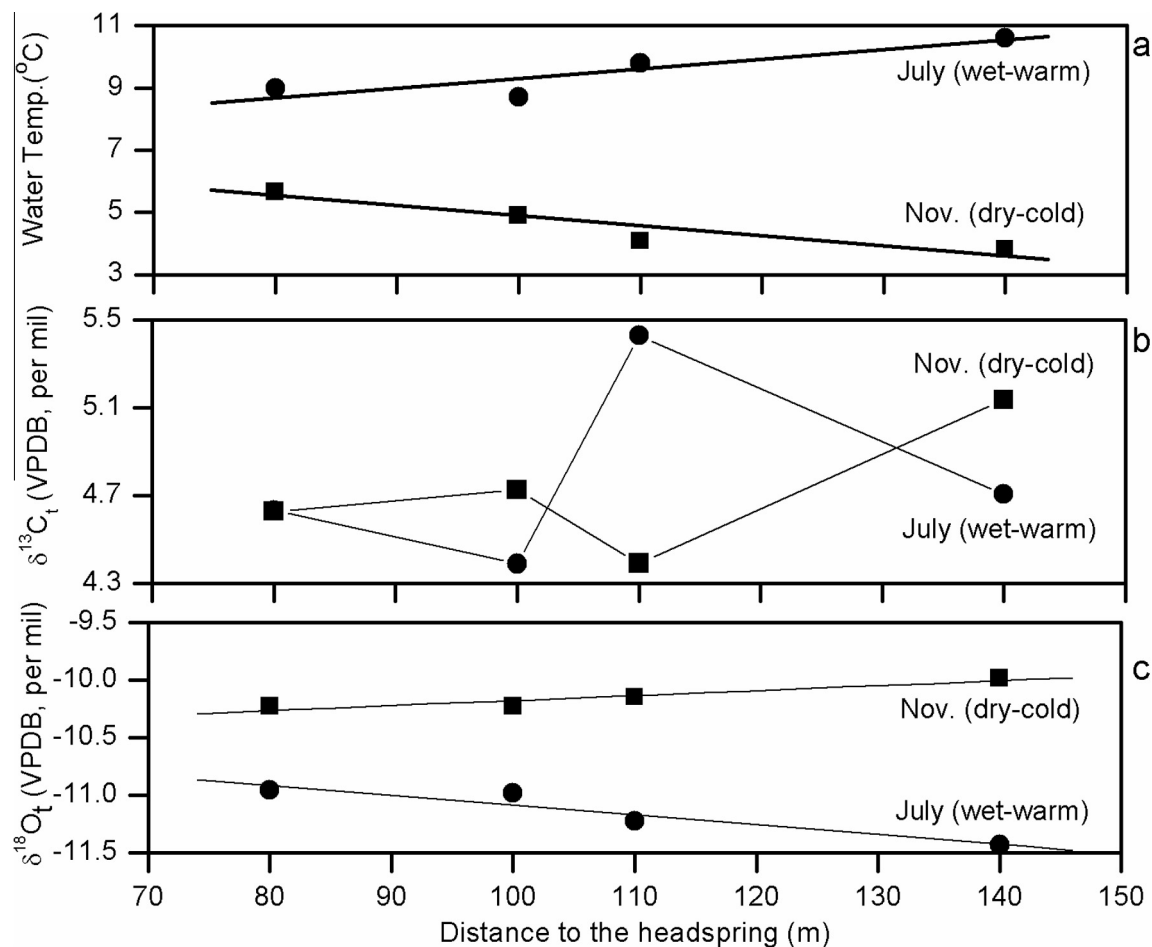


Fig. 7. Spatial variation in the $\delta^{13}C$ (b) and $\delta^{18}O$ (c) values of pool travertine under wet (July) and dry (November) conditions at Huanglong Ravine, in relation to changes in the coeval water temperature (a).

When deposition is in isotopic equilibrium the $\delta^{13}C$ value of travertine is correlated with that of dissolved carbonate (mainly as bicarbonate) in the solution. Here in Matihai ramp section, the bicarbonate in the solution is supplied by both groundwater and overland flow. The former was stable in our study because the CO_2 source at the Ravine was primarily endogenic, while the latter varied with the rainfall. As noted, the climate at Huanglong Ravine is typical subtropical monsoon with about 72% of the annual precipitation occurring during the rainy season from May to September. In that season, abundant overland flow supplied by rainwater and soil water with low $\delta^{13}C$ values recharged the stream, resulting in a decrease in the $\delta^{13}C$ values of bicarbonate and thus of travertine. In addition, inputs of overland flow into the stream decreased the pCO_2 in the solution (Fig. 3b), reducing degassing of CO_2 from water to the atmosphere, which will also lead to lower $\delta^{13}C$ values in the dissolved carbonate. Therefore, the lower $\delta^{13}C$ values of the travertine in the rainy season result from the combination of “isotopic dilution” by overland flow with lower $\delta^{13}C$ values and the lower pCO_2 in the solution. The dilution effect is evidenced by the lower $\delta^{13}C$ values of ramp travertine taken in July compared to November (Fig. 6b), and the effect of slower CO_2 -degassing from water

can be seen from different pCO_2 (Fig. 3) and the differing slopes in July and November in Fig. 6b. The steeper slope indicates accelerated degassing of CO_2 when the water flows downstream in the dry season (November). The negative effect of flow rate on degassing of CO_2 was also found in other travertine/tufa sites (Hori et al., 2009; Sun and Liu, 2010). The greater the water flow rate is, the less the amount of CO_2 per unit volume of water degasses (Hori et al., 2009).

When deposited in isotopic equilibrium, the $\delta^{18}O$ value of travertine is determined not only by the $\delta^{18}O$ value of parent water but also by water temperature. The $\delta^{18}O$ values of rainwater at Huanglong Ravine displayed a seasonal change, i.e., lower in the rainy season and higher in the dry season (Wang et al., 2012). This resulted in similar variation pattern in the $\delta^{18}O$ values of overland flow supplied by rainfall and snowmelt water. In the rainy season, overland flow with low $\delta^{18}O$ values entered the ramp stream, decreasing the $\delta^{18}O$ values of water. In addition, higher temperatures in the rainy season reduced the isotopic fractionation, also lowering $\delta^{18}O$ values of the travertine precipitated. Together these two processes resulted in lower $\delta^{18}O$ values of ramp travertine in the wet season than in the dry (Fig. 6c). However, the $\delta^{18}O$ values of travertine did not

Table 4

The measured and theoretical equilibrium fractionations ($\Delta^{18}\text{O}_{\text{t-water}}$), the latter calculated by using the mean values of water temperature during each experimental run (~ 10 days) at the Matihai ramp (Site No. 2) and the equations of Kim and O'Neil (1997) and Coplen (2007).

Date	Site	Mean water temperature (VPDB. ‰)	$\delta^{13}\text{C}_t$ (VPDB. ‰)	$\delta^{18}\text{O}_t$ (VPDB. ‰)	$\delta^{18}\text{O}_t$ (VSMOW. ‰)	$\delta^{18}\text{O}_{\text{water}}$ (VSMOW. ‰)	$\Delta^{18}\text{O}_{\text{t-water}}$ (VSMOW. ‰)	Theoretical $\Delta^{18}\text{O}_{\text{t-water}}^a$ (VSMOW. ‰)	Theoretical $\Delta^{18}\text{O}_{\text{t-water}}^b$ (VSMOW. ‰)
2010/6/2	Site No. 2	5.9	2.73	-10.05	20.55	-11.42	31.97	32.23	33.79
2010/6/12		6.0	2.24	-10.22	20.37	-11.20	31.57	32.20	33.77
2010/6/26		7.6	-	-	-	-11.32	-	31.84	33.41
2010/7/7		7.3	3.61	-9.82	20.79	-11.96	32.75	31.90	33.48
2010/7/17		6.5	3.48	-	20.40	-11.83	-	32.09	33.65
2010/7/28		10.7	-	-10.19	-	-11.52	31.92	31.13	32.73
2010/8/8		12.9	4.55	-10.13	20.47	-11.80	32.27	30.64	32.26
2010/8/19		11.0	-	-	-	-11.46	-	31.07	32.67
2010/8/29		8.1	3.68	-10.42	20.17	-12.09	32.27	31.72	33.30
2010/9/8		8.7	3.69	-10.32	20.27	-11.61	31.88	31.58	33.17
2010/9/18		9.6	3.77	-10.31	20.28	-12.10	32.38	31.38	32.97
2010/9/28		7.8	4.24	-9.90	20.71	-12.17	32.88	31.79	33.37
2010/10/8		7.3	4.01	-10.21	20.38	-12.07	32.46	31.90	33.48
2010/10/18		8.3	4.73	-9.69	20.92	-11.84	32.75	31.68	33.26
2010/10/28		6.8	4.95	-9.82	20.79	-12.01	32.79	32.02	33.59
2010/11/6		6.2	5.30	-9.66	20.95	-11.80	32.75	32.16	33.72

^a Theoretical equilibrium fractionations ($\Delta^{18}\text{O}_{\text{t-water}}$) by using the equation of Kim and O'Neil (1997);

^b Theoretical equilibrium fractionations ($\Delta^{18}\text{O}_{\text{t-water}}$) by using the equation of Coplen (2007).

show significant correlation with either water temperature or rainfall ($R = -0.40$ and -0.19 , respectively, Table 3), indicating that there may be other factor(s) controlling the $\delta^{18}\text{O}$ of the travertine. Yan et al. (2012) found that $\delta^{18}\text{O}$ values of travertine in rapid flow systems were easily affected by kinetic fractionation. Here, the mean water temperatures during each 10 days' experimental period at Site No. 2 were used to calculate the theoretical fractionation between travertine and water using the equations of Kim and O'Neil (1997) and Coplen (2007) to check if oxygen isotopic equilibrium was achieved (Table 4 and Fig. 8). It can be seen that the measured fractionation between travertine and water located between the fractionation lines raised by Kim and O'Neil (1997) and Coplen (2007). Recent studies (Dietzel et al., 2009; Day and Henderson, 2011; Feng et al., 2012) suggested that actual equilibrium fractionation is larger than those derived by Kim and O'Neil (1997) and closer to those by Coplen (2007). The $\delta^{18}\text{O}$ values lower than those predicted by Coplen (2007) may be explained by preferred incorporation of ^{16}O over ^{18}O in the solid carbonate due to surface entrapment (Watson, 2004; Day and Henderson, 2011).

In addition, spatially increasing trends in $\delta^{18}\text{O}$ values of travertine were recorded in both wet and dry season (Fig. 6c), while water temperature increased downstream in the summer season only. This is similar to another travertine-depositing canal at Baishuitai, SW China, where $\delta^{18}\text{O}$ values of travertine and water temperature increased downstream while $\delta^{18}\text{O}$ values of water stayed stable (Yan et al., 2012). The authors suggested that this is due to Rayleigh fractionation by incomplete exchange of oxygen isotope between HCO_3^- and H_2O when travertine deposited fast. Similarly, the spatially synchronous increase of $\delta^{18}\text{O}$ and $\delta^{13}\text{C}$ values during different depositing periods ($R = 0.66$ in July and 0.79 in November) seems to be an

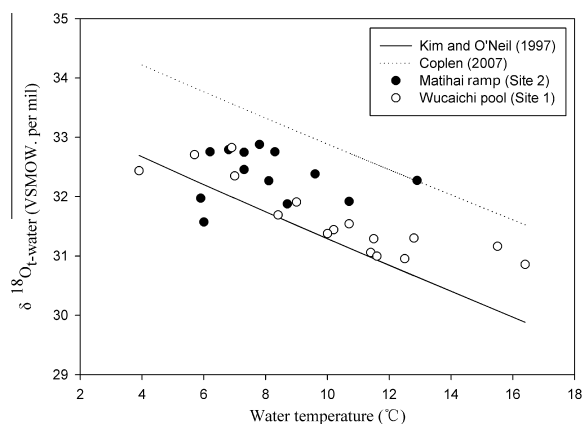


Fig. 8. Oxygen isotopes fractionation between travertine and water vs. water temperature. The measured fractionations at Wucaichi pool (Site 1) and Matihai ramp (Site 2) are shown together with two theoretical equilibrium curves based on the equations of Kim and O'Neil (1997) and Coplen (2007), respectively.

evidence of kinetic fractionation too (Hendy, 1971; Dreybrodt and Scholz, 2011).

It is therefore concluded that the $\delta^{13}\text{C}$ values of the ramp travertine were related to the amounts of rain falling in Huanglong Ravine while the $\delta^{18}\text{O}$ values of travertine here were affected by combined effect of rainfall, water temperature and kinetic fractionation. Temporally, the $\delta^{13}\text{C}$ and $\delta^{18}\text{O}$ values of the ramp travertine showed a weak positive correlation with each other (Fig. 9a). Due to the negative correlation between $\delta^{13}\text{C}$ values and rainfall (Fig. 10a), one could reconstruct the paleo-rainfall at Huanglong Ravine by using the $\delta^{13}\text{C}$ values of fossil ramp travertine deposited here. In Fig. 10a, the correlation coefficient

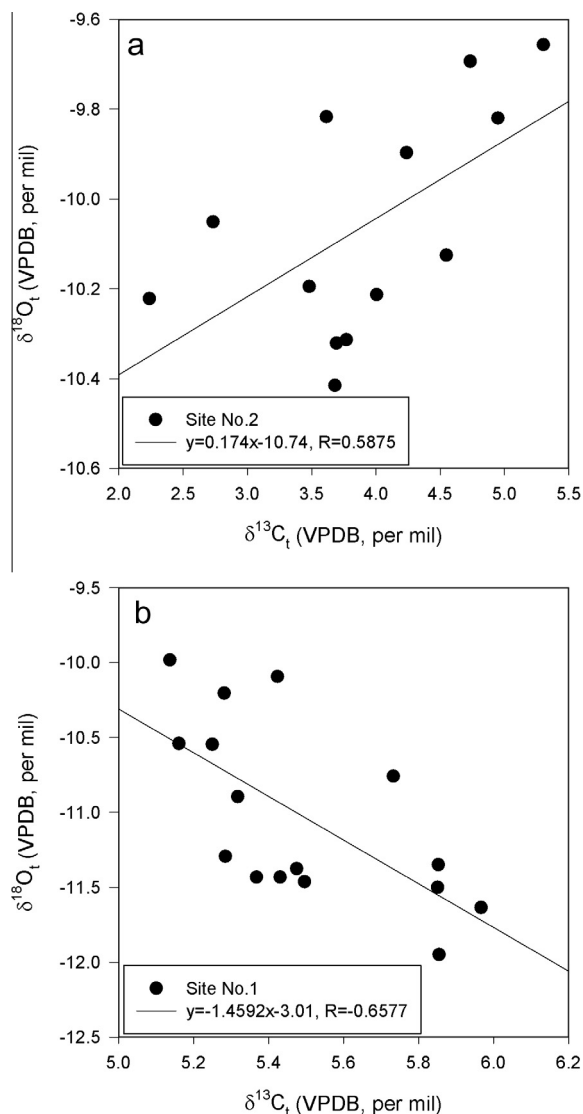


Fig. 9. Plots of $\delta^{13}C$ v $\delta^{18}O$ values of the modern endogene travertine at the Sites No. 1 (b) and 2 (a).

between travertine $\delta^{13}C$ values and rainfall is relatively low ($R = -0.68$). One possible reason for this is that total amount of rainfall during each experimental run (~ 10 days) was chosen for calculation of correlation coefficient (Fig. 10a). However, the dilution effects of the surface flow may not synchronize with each rain event. In other words, dilution effects of surface flow usually lag behind rain event. This would reduce the correlation coefficient between travertine $\delta^{13}C$ values and rainfall in Fig. 10a. To evaluate the actual relationship between travertine $\delta^{13}C$ values and rainfall, concentration of SO_4^{2-} in the water was chosen (Table 5). According to Yoshimura et al. (2004), SO_4^{2-} is mainly from sulfuric acid underground. So SO_4^{2-} seems to be an ideal index to determine the proportion of overland flow thus the dilution effect caused by rain. The correlation coefficient between travertine $\delta^{13}C$ values and concentration of SO_4^{2-} was 0.82, higher than that in Fig. 10a. Anyway, to obtain precise values of local rainfall by using $\delta^{13}C$ values of

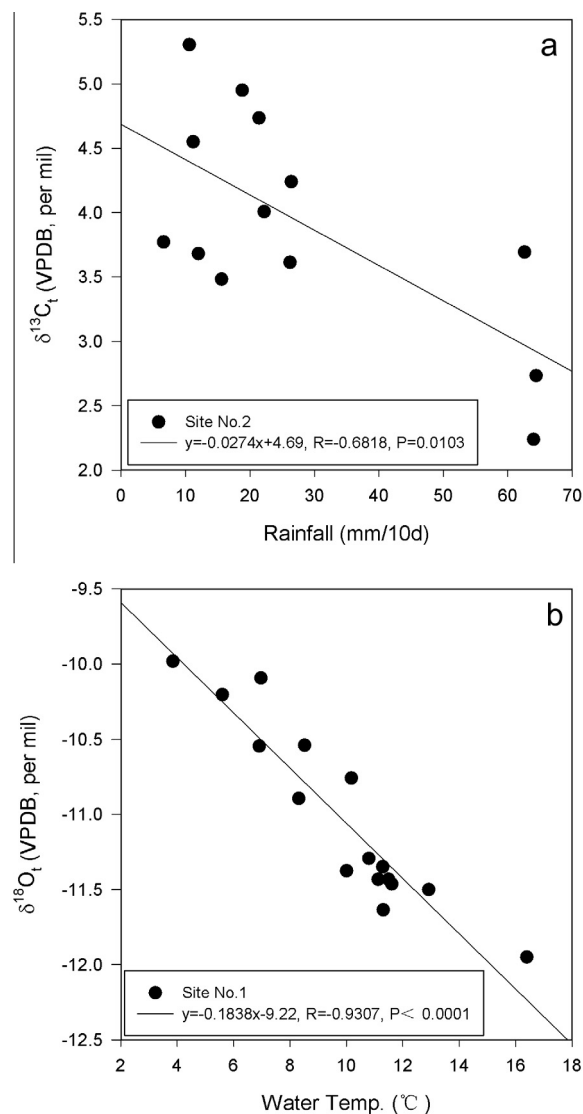


Fig. 10. (a) Relationship between the ramp travertine $\delta^{13}C$ values and coeval total rainfall during each experimental run (~ 10 days) at Site No. 2; (b) Relationship between the pool travertine $\delta^{18}O$ values and coeval mean water temperature during each experimental run (~ 10 days) at Site No. 1.

travertine at the ramp section, more data by long-time monitoring and sampling are needed to improve this correlation relationship. Moreover, it should be emphasized that the hydrology of Matihai ramp section in Huanglong Ravine is specialized due to mixture of groundwater and surface water. So, the negative relationship between $\delta^{13}C$ values of travertine and rainfall could only be applied to tropical seasonal systems where the “isotopic dilution effect” is strong.

5.2. Temperature effects on variations in the $\delta^{13}C$ and $\delta^{18}O$ values of the pool travertine: implications for estimation of paleotemperature

When a carbonate is deposited in isotopic equilibrium, the $\delta^{18}O$ value is determined both by temperature and the $\delta^{18}O$ of the parent water (Kim and O’Neil, 1997). This

Table 5

Concentrations of minor ions in the water at Wucaichi pool (Site No. 1) and Matihai ramp (Site No. 2) in Huanglong Ravine (unit: mg/L).

Date	Site	K ⁺	Na ⁺	Mg ²⁺	Cl ⁻	SO ₄ ²⁻	Site	K ⁺	Na ⁺	Mg ²⁺	Cl ⁻	SO ₄ ²⁻
2010/5/26	Site No.1	0.32	2.35	20.69	0.55	26.73	Site No. 2	0.13	1.36	11.97	0.23	23.62
2010/6/2		0.36	2.42	20.64	0.64	25.11		0.12	1.35	10.72	0.39	17.64
2010/6/12		0.31	2.40	20.30	0.59	24.63		0.13	1.39	10.55	0.33	16.71
2010/6/25		0.28	2.30	20.19	0.44	25.21		0.12	1.49	12.52	0.49	19.51
2010/7/7		0.30	2.31	20.63	0.47	24.89		0.10	1.18	10.55	0.37	18.58
2010/7/16		0.29	2.40	21.06	0.67	25.00		0.13	1.41	11.88	0.38	19.35
2010/7/28		0.34	2.50	21.78	0.75	26.65		0.14	1.59	12.86	0.32	21.27
2010/8/8		0.34	2.52	21.65	0.63	26.82		0.19	1.80	13.88	0.60	22.98
2010/8/19		0.29	2.23	20.26	0.26	24.95		0.14	1.27	11.31	0.25	22.10
2010/8/29		0.33	2.45	21.56	0.81	26.37		0.15	1.59	13.03	0.33	22.00
2010/9/8		0.34	2.41	21.22	0.50	27.57		0.14	1.51	12.23	0.13	24.85
2010/9/18		0.35	2.41	21.32	0.78	27.10		0.16	1.68	13.45	0.31	23.45
2010/9/27		0.31	2.23	20.44	0.35	27.38		0.19	1.36	14.72	0.45	24.41
2010/10/7		0.33	2.27	20.68	0.56	27.58		0.21	1.33	13.87	0.52	25.15
2010/10/17		0.30	2.21	20.50	0.64	28.07		0.20	1.41	14.76	0.30	25.53
2010/10/27		0.32	2.21	19.84	1.53	27.38		0.20	1.45	15.48	0.71	25.14

provides a basis for researchers to reconstruct paleo-temperature by using $\delta^{18}\text{O}$ values of carbonate sediments such as tufa and travertine.

Matsuoka et al. (2001) found that the $\delta^{18}\text{O}$ curves in Japanese laminated tufas reflect seasonal changes in water temperature while the $\delta^{18}\text{O}$ values of stream water remained relatively stable over time. Yan et al. (2012) investigated the oxygen isotopes in two travertine-depositing systems with differing hydrodynamic conditions at Baishuitai, Yunnan, SW China. They suggested that variation of the $\delta^{18}\text{O}$ values of travertine deposited in pools reflected the change in water temperature, while $\delta^{18}\text{O}$ values of travertine deposited in a canal were mainly controlled by kinetic fractionation due to rapid deposition rates.

It can be seen that the $\delta^{18}\text{O}$ values of travertine at Site 1 (the Wucaichi Pools) in this study showed anti-phase change with water temperature (Fig. 4). The linear correlation between travertine $\delta^{18}\text{O}$ and water temperature is shown in Fig. 10b. The high correlation coefficient ($R = -0.93$, Table 3) indicates the strong temperature effect on the isotopic fractionation i.e., the higher temperature results in the lower $\delta^{18}\text{O}$ value. Meanwhile, downstream spatial variations of travertine $\delta^{18}\text{O}$ value through the pools show anti-phase change with water temperature in both wet and dry seasons (Fig. 7c vs. 7a). This further suggested that water temperature change was the main factor governing the variation of $\delta^{18}\text{O}$ values of travertine in Wucaichi Pools at Huanglong Ravine. To check if oxygen isotopic equilibrium between travertine and water was achieved, the mean water temperatures during each experimental run (~10 days) at Site No. 1 were used to calculate the theoretical fractionation using the equations of Kim and O'Neil (1997) and Coplen (2007) (Table 6 and Fig. 8). Similar to Matihai ramp section, measured fractionations were also between the fractionation lines raised by Kim and O'Neil (1997) and Coplen (2007). However, though $\delta^{18}\text{O}$ values of travertine at Site No. 1 were affected by kinetic effect due to surface entrapment suggested by Feng et al. (2012), $\delta^{18}\text{O}$ values showed significant correlation with water temperature. One possible explanation is that the

kinetic fractionation did not change during the study period. Dietzel et al. (2009) and Feng et al. (2012) found there is a relationship between kinetic fractionation and calcite precipitation rates. For Site No. 1 in this study, travertine had a much narrower range of precipitation rates during the study period (Table 7). The second explanation is that the equilibrium fractionation of oxygen isotope between HCO_3^- and H_2O is achieved. Because of the negative correlation between oxygen isotopic fractionation of the dissolved carbonate species and water and temperature (Beck et al., 2005), some travertine out of equilibrium may still have the potential for paleo-temperature reconstruction (Yan et al., 2012). In a word, one can reconstruct paleo-temperature by using the $\delta^{18}\text{O}$ values of travertine deposited in the pools at the Site 1.

$\delta^{13}\text{C}$ values of pool travertine showed a weak positive relation with water temperature (Table 3 and Fig. 4). One reason may be that equilibrium fractionation during calcite precipitation led to the lower $\delta^{13}\text{C}$ values in the pool travertine in winter and higher in summer (Mook and de Vries, 2001). On the other hand, higher temperature facilitates the degassing of CO_2 to the atmosphere. This is evidenced by the positive correlation between pCO_2 and water temperature (Fig. 3a, $R = 0.74$). Higher pCO_2 and higher temperature increased degassing rate of CO_2 , leaving the isotopically heavier carbonates in solution and thus in travertine. Due to these combined effects, $\delta^{13}\text{C}$ values are negatively correlated with $\delta^{18}\text{O}$ values in travertine deposited in the pools (Fig. 9b), quite different from the relationship found in the ramp stream system (Fig. 9a).

5.3. The importance of identifying the depositional environment of fossil travertine before using it to reconstruct paleoclimate

The different mechanisms responsible for variations in the $\delta^{18}\text{O}$ and $\delta^{13}\text{C}$ values of travertine deposited in the two subsystems (pool and stream) resulted in different relationships between travertine $\delta^{18}\text{O}$ and $\delta^{13}\text{C}$ values and pertinent climatic parameters (rainfall and temperature).

Table 6

The measured and theoretical equilibrium fractionations ($\Delta^{18}\text{O}_{\text{t-water}}$), the latter calculated by using the mean values of water temperature during each experimental run (~10 days) at the Wucaichi pool (Site No. 1) and the equations of Kim and O'Neil (1997) and Coplen (2007).

Date	Site	Mean water temperature	$\delta^{13}\text{C}_t$ (VPDB. ‰)	$\delta^{18}\text{O}_t$ (VPDB. ‰)	$\delta^{18}\text{O}_t$ (VSMOW. ‰)	$\delta^{18}\text{O}_{\text{water}}$ (VSMOW. ‰)	$\Delta^{18}\text{O}_{\text{t-water}}$ (VSMOW. ‰)	Theoretical $\Delta^{18}\text{O}_{\text{t-water}}$ ^a (VSMOW. ‰)	Theoretical $\Delta^{18}\text{O}_{\text{t-water}}$ ^b (VSMOW. ‰)
2010/6/2	NO. 1	10.2	5.48	-11.38	19.18	-12.26	31.44	31.25	32.84
2010/6/12		8.4	5.16	-10.54	20.04	-11.65	31.69	31.65	33.23
2010/6/26		10.0	5.73	-10.76	19.82	-11.56	31.38	31.29	32.88
2010/7/7		11.4	5.50	-11.46	19.09	-11.97	31.06	30.98	32.58
2010/7/17		10.7	5.29	-11.29	19.27	-12.27	31.54	31.13	32.73
2010/7/28		12.5	5.43	-11.43	19.12	-11.83	30.95	30.73	32.35
2010/8/8		16.4	5.86	-11.95	18.59	-12.27	30.86	29.88	31.52
2010/8/19		15.5	5.97	-11.64	18.91	-12.25	31.16	30.08	31.71
2010/8/29		11.5	5.37	-11.43	19.12	-12.16	31.29	30.95	32.56
2010/9/8		11.6	5.85	-11.35	19.21	-11.79	31.00	30.93	32.54
2010/9/18		12.8	5.85	-11.50	19.05	-12.25	31.30	30.67	32.28
2010/9/28		9.0	5.32	-10.89	19.68	-12.23	31.91	31.52	33.10
2010/10/8		6.9	5.42	-10.09	20.50	-12.32	32.83	32.00	33.57
2010/10/18		7.0	5.25	-10.55	20.04	-12.31	32.35	31.97	33.54
2010/10/28		5.7	5.28	-10.20	20.39	-12.32	32.71	32.27	33.83
2010/11/6		3.9	5.14	-9.98	20.62	-11.82	32.44	32.69	34.24

^a Theoretical equilibrium fractionations ($\Delta^{18}\text{O}_{\text{t-water}}$) by using the equation of Kim and O'Neil (1997).

^b Theoretical equilibrium fractionations ($\Delta^{18}\text{O}_{\text{t-water}}$) by using the equation of Coplen (2007).

Table 7

The travertine precipitation rates at Wucaichi pool (Site No. 1) and Matihai ramp (Site No. 2) during the each sampling run.

Sampling date	Precipitation rates at Site No. 1 (mg cm ⁻² d ⁻¹)	Precipitation rates at Site No. 2 (mg cm ⁻² d ⁻¹)
2010/6/2	0.59	0.18
2010/6/12	0.59	–
2010/6/26	0.72	0.90
2010/7/7	0.75	0.45
2010/7/17	0.68	–
2010/7/28	0.32	0.79
2010/8/8	0.37	1.09
2010/8/19	0.73	1.07
2010/8/29	0.61	0.19
2010/9/8	0.71	0.91
2010/9/18	0.62	0.72
2010/9/28	0.61	1.00
2010/10/8	0.56	0.68
2010/10/18	0.56	0.40
2010/10/28	0.48	0.31
Average	0.59	0.67

–: No data due to sample lost.

Therefore, an important step is to identify the depositional environment of fossil travertines before using them to reconstruct paleoclimate (Andrews et al., 1997). First, morphological investigations are needed to check if the travertine formed in a pool system, where it is characterized by very regular, thin and largely monochrome (Yan et al., 2012), or deposited in a ramp stream system with distinct alternative darker and lighter colored layers due to the overland flow which carries much clays and/or organic matter (Liu et al., 2010). Second, in pool travertine the $\delta^{18}\text{O}$ shows a generally negative relationship with the $\delta^{13}\text{C}$, while there is a positive relationship between $\delta^{18}\text{O}$ and $\delta^{13}\text{C}$ in ramp deposits.

In a word, travertines deposited under different hydrodynamic conditions have different composition, which must be examined before using them to reconstruct paleoclimatic parameters.

6. CONCLUSIONS

Temporal and spatial variations in the $\delta^{13}\text{C}$ and $\delta^{18}\text{O}$ values of travertines being deposited today in Huanglong Ravine were examined to understand the potential of older deposits for paleoclimatic and paleoenvironmental interpretations. It was found that $\delta^{13}\text{C}$ and $\delta^{18}\text{O}$ in travertine formed in a ramp stream were depleted in the warm rainy season and enriched in the cold dry season. The positive correlation was mainly caused by dilution and rainfall seasonal effects on the $\delta^{13}\text{C}$ and $\delta^{18}\text{O}$ respectively, i.e., low $\delta^{13}\text{C}$ values were caused by dilution by overland flow with depleted $\delta^{13}\text{C}$ values and reduced CO_2 -degassing in the warm rainy season while low $\delta^{18}\text{O}$ values of travertine were because of low $\delta^{18}\text{O}$ values of water induced by seasonal variation in oxygen isotopic ratios of rainwater. Meanwhile, kinetic effect on oxygen isotopic fractionation during ramp travertine deposition existed and reduced this positive correlation. In contrast, the $\delta^{13}\text{C}$ and $\delta^{18}\text{O}$ values of the pool travertines showed converse changes, which were caused by the temperature effect. Low $\delta^{18}\text{O}$ values and high $\delta^{13}\text{C}$ values in the warm rainy season chiefly reflect the higher water temperatures. Therefore, both the $\delta^{13}\text{C}$ and $\delta^{18}\text{O}$ values may be used for paleo-rainfall and/or paleo-temperature reconstruction where one knows the $\delta^{13}\text{C}$ and $\delta^{18}\text{O}$ values of the fossil endogenic travertine at Huanglong Ravine. Though these patterns were found in systems with a pronounced rainy period where the isotopic amount effect is strong, we think oxygen isotopes between water and bicarbonate achieve equilibrium easily in pools, so the

former conclusion on oxygen isotope may be applicable to any area where strong evaporation doesn't exist. For example, similar case was also found from another travertine site at Baishuitai, SW China (Yan et al., 2012). However, it should be emphasized that the hydrology of Matihai ramp section in Huanglong Ravine is specialized due to mixture of groundwater and surface water. So, the negative relationship between $\delta^{13}\text{C}$ values of travertine and rainfall could only be applied to tropical seasonal systems where the "isotopic dilution effect" is strong.

This study thus demonstrates that endogenic travertine, like epigenic (meteoene) tufa, may be a good candidate for high-resolution paleoclimatic and paleoenvironmental reconstructions. However, since travertines deposited under different hydrodynamic conditions have differing isotopic responses to climate parameters, it is necessary to check the depositional facies of fossil travertine samples before they can be used for palaeoclimate reconstruction (Andrews et al., 1997).

ACKNOWLEDGMENTS

This work was supported by the National Natural Science Foundation of China (Grant Nos. 41172232) and the 973 Program of China (2013CB956703). Special thanks are given to Derek Ford (McMaster University, Canada), the three anonymous reviewers and the associate editor for their thoughtful comments and suggestions, which greatly improved the original draft.

REFERENCES

- Andrews J. E. (2006) Palaeoclimatic records from stable isotopes in riverine tufas: synthesis and review. *Earth Sci. Rev.* **75**, 85–104.
- Andrews J. E. and Brasier A. T. (2005) Seasonal records of climatic change in annually laminated tufas: short review and future prospects. *J. Quat. Sci.* **20**, 411–421.
- Andrews J. E., Riding R. and Dennis P. F. (1997) The stable isotope record of environmental and climatic signals in modern terrestrial microbial carbonates from Europe. *Palaeogeogr. Palaeoclimatol. Palaeoecol.* **129**, 171–189.
- Beck W. C., Grossman E. L. and Morse J. W. (2005) Experimental studies of oxygen isotope fractionation in the carbonic acid system at 15, 25, and 40 °C. *Geochim. Cosmochim. Acta* **69**, 3493–3503.
- Coplen T. B. (2007) Calibration of the calcite–water oxygen isotope geothermometer at Devils Hole, Nevada, a natural laboratory. *Geochim. Cosmochim. Acta* **71**, 3948–3957.
- Day C. C. and Henderson G. M. (2011) Oxygen isotopes in calcite grown under cave-analogue conditions. *Geochim. Cosmochim. Acta* **75**, 3956–3972.
- Dreybrodt W. and Scholz D. (2011) Climatic dependence of stable carbon and oxygen isotope signals recorded in speleothems: from soil water to speleothem calcite. *Geochim. Cosmochim. Acta* **75**, 734–752.
- Dietzel M., Tang J., Leis A. and Kohler S. J. (2009) Oxygen isotopic fractionation during inorganic calcite precipitation—effects of temperature, precipitation rate and pH. *Chem. Geol.* **268**, 107–115.
- Feng W., Banner J. L., Guilfoyle A. L., Musgrove M. and James E. W. (2012) Oxygen isotopic fractionation between drip water and speleothem calcite: a 10-year monitoring study, central Texas USA. *Chem. Geol.* **304–305**, 53–67.
- Hendy C. H. (1971) The isotopic geochemistry of speleothems: I. The calculation of effects of different modes of formation on the isotopic composition of speleothems and their applicability as paleoclimatic indicators. *Geochim. Cosmochim. Acta* **35**, 801–824.
- Hori M., Kawai T., Matsuoka J. and Kano A. (2009) Intra-annual perturbations of stable isotopes in tufas: effects of hydrological processes. *Geochim. Cosmochim. Acta* **73**, 1684–1695.
- Kano A., Matsuoka J., Kojo T. and Fujii H. (2003) Origin of annual laminations in tufa deposits, southwest Japan. *Palaeogeogr. Palaeoclimatol. Palaeoecol.* **191**, 243–262.
- Kawai T., Kano A. and Hori M. (2009) Geochemical and hydrological controls on biannual lamination of tufa deposits. *Sediment. Geol.* **213**, 41–50.
- Kim S. T. and O'Neil J. R. (1997) Equilibrium and nonequilibrium oxygen isotope effects in synthetic carbonates. *Geochim. Cosmochim. Acta* **61**, 3461–3475.
- Krawczyk W. E. and Ford D. C. (2006) Correlating specific conductivity with total hardness in limestone and dolomite karst waters. *Earth Surf. Process. Landforms* **31**, 221–234.
- Liu Z., Svensson U., Dreybrodt W., Yuan D. and Buhmann D. (1995) Hydrodynamic control of inorganic calcite precipitation in Huanglong Ravine, China: field measurements and theoretical prediction of deposition rates. *Geochim. Cosmochim. Acta* **59**, 3087–3097.
- Liu Z., Yuan D., He S., Zhang M. and Zhang J. (2000) Geochemical features of the geothermal CO₂–water–carbonate rock system and analysis on its CO₂ sources. *Sci. China* **43**, 569–576.
- Liu Z., Groves C., Yuan D., Meiman J., Jiang G. and He S. (2004) Hydrochemical variations during flood pulses in the southwest China peak cluster karst: Impacts of CaCO₃–H₂O–CO₂ interactions. *Hydrol. Process.* **18**, 2423–2437.
- Liu Z., Li H., You C., Wan N. and Sun H. (2006) Thickness and stable isotopic characteristics of modern seasonal climate-controlled sub-annual travertine laminas in a travertine-depositing stream at Baishuitai, SW China: implications for paleoclimate reconstruction. *Environ. Geol.* **51**, 257–265.
- Liu Z., Sun H., Lu B., Liu X., Ye W. and Zeng C. (2010) Wet-dry seasonal variations of hydrochemistry and carbonate precipitation rates in a travertine-depositing canal at Baishuitai, Yunnan, SW China: implications for the formation of biannual laminae in travertine and for climatic reconstruction. *Chem. Geol.* **273**, 258–266.
- Matsuoka J., Kano A., Oba T., Watanabe T., Sakai S. and Seto K. (2001) Seasonal variation of stable isotopic compositions recorded in a laminated tufa SW Japan. *Earth Planet. Sci. Lett.* **192**, 31–44.
- McDermott F. (2004) Palaeo-climate reconstruction from stable isotope variations in speleothems: a review. *Quat. Sci. Rev.* **23**, 901–918.
- Mook W. G. and de Vries J. J. (2001) Environmental isotopes in the hydrological cycle. In *Principles and Application. Volume I: Introduction, Theory, Methods, Review* (ed. W. G. Mook). UNESCO/IAEA, Vienna, Austria and Paris France. pp. 1–280.
- Sun H. and Liu Z. (2010) Wet–dry seasonal and spatial variations in the $\delta^{13}\text{C}$ and $\delta^{18}\text{O}$ values of the modern endogenic travertine at Baishuitai, Yunnan, SW China and their paleoclimatic and paleoenvironmental implications. *Geochim. Cosmochim. Acta* **74**, 1016–1029.
- Wang Y., Cheng H., Edwards R. L., An Z., Wu J., Shen C. and Dorale J. A. (2001) A high-resolution absolute-dated Late Pleistocene monsoon record from Hulu Cave, China. *Science* **294**, 2345–2348.
- Wang Y., Cheng H., Edwards R. L., Kong X., Shao X., Chen S., Wu J., Jiang X., Wang X. and An Z. (2008) Millennial- and

- orbital-scale changes in the East Asian monsoon over the past 224,000 years. *Nature* **451**, 1090–1093.
- Wang H., Liu Z., Zhang J., Sun H., An D., Fu R. and Wang X. (2010) Spatial and temporal hydrochemical variation of the spring-fed travertine-deposition stream in the Huanglong Ravine, Sichuan SW China. *Acta Carsol.* **39**, 247–259.
- Wang H., Zhang J. and Liu Z. (2012) Indications of the hydrogen and oxygen isotopes in precipitation for climate change in Huanglong Sichuan. *Carsol. Sinica* **31**, 25–30 (in Chinese with English abstract).
- Watson E. B. (2004) A conceptual model for near-surface kinetic controls on the trace-element and stable isotope composition of abiogenic calcite crystals. *Geochim. Cosmochim. Acta* **68**, 1473–1488.
- Yan H., Sun H. and Liu Z. (2012) Equilibrium vs. kinetic fractionation of oxygen isotopes in the two low-temperature travertine-depositing systems with distinct hydrodynamic conditions at Baishuitai, Yunnan SW China. *Geochim. Cosmochim. Acta* **95**, 63–78.
- Yoshimura K., Liu Z., Cao J., Yuan D., Inokura Y. and Noto M. (2004) Deep source CO₂ in natural waters and its role in extensive tufa deposition in the Huanglong Ravines, Sichuan China. *Chem. Geol.* **205**, 141–153.
- Yuan D., Cheng H., Edwards R. L., Dykoski C. A., Kelly M. J., Zhang M., Qing J., Lin Y., Wang Y., Wu J., Dorale J. A., An Z. and Cai Y. (2004) Timing, duration, and transitions of the last interglacial Asian monsoon. *Science* **304**, 575–578.
- Zhang X., Nakawo M., Yao T., Han J. and Xie Z. (2002) Variations of stable isotopic compositions in precipitation on the Tibetan Plateau and its adjacent regions. *Sci. China* **45**, 481–493.
- Zhang J., Wang H., Liu Z., An D. and Dreybrodt W. (2012) Spatial-temporal variations of travertine deposition rates and their controlling factors in Huanglong Ravine, China – a world's heritage site. *Appl. Geochem.* **27**, 211–222.

Associate editor: Miryam Bar-Matthews